Radioprotection 2018, 54(2), 133–140
© EDP Sciences 2019
https://doi.org/10.1051/radiopro/2019006

Available online at:
www.radioprotection.org

ARTICLE

Calculation of self-absorption and coincidence summing correction factors for the extended sources using GEANT4

W. Khan, C. He* and Y. Cao

Department of Nuclear Science and Technology, School of Energy and Power Engineering, Xi'an Jiaotong University, Xi'an 710049, PR China.

Received: 27 September 2018 / Accepted: 12 February 2019

Abstract – A detailed study of the full energy peak efficiency of a high purity germanium (HPGe) detector including the effect of source self-absorption and coincidence summing was performed using Monte Carlo simulation, as it is difficult and time-consuming to measure the full energy peak efficiency experimentally. Cylindrical water composition source was simulated with different characteristics, covering the energy range from 60 to 1836 keV. Self-absorption correction factors (SAF_{cal}) were calculated for two source volumes and obtained good agreement with the experimental results except for (^{60}Co and ^{88}Y) nuclides. The simulation was performed for various samples with different densities and observed their effects on the full energy peak efficiency value of the detector. In the case of extended volumetric source, the coincidence summing correction factors (CSF_{cal}) for two nuclides (^{60}Co and ^{88}Y) were estimated with the GEANT4 simulation toolkit. The effect of correction factors on different cylindrical source volumes was also investigated. With the self-absorption and coincidence summing effect, the best agreement was achieved between simulated and experimental results with discrepancy less than 2% for all of the radionuclides included in two source volumes.

Keywords: GEANT4 / HPGe detector / full energy peak efficiency / self-absorption / coincidence summing / cylindrical sources

1 Introduction

γ-ray spectrometry with high purity germanium detectors (HPGe) is widely used for determining the concentration and identification of unknown radionuclides in environmental samples. To determine the activity of each radionuclide, it is necessary to calculate the full energy peak efficiency at the energy of γ-ray emissions for a given measuring geometry. Most of the authors used different approaches and methods to calibrate HPGe detector efficiency (Helmer *et al.*, 2004; Hurtado *et al.*, 2004; Budjáš *et al.*, 2009; Conti *et al.*, 2013). But the major problem for HPGe detector efficiency calibration with environmental samples is the extended source dimension and self-absorption of the source matrix. However, the extended source dimension is not a significant problem because the average path length traveled by a photon inside the source matrix but photon absorption within the sample itself is difficult to achieve. For this reason, several procedures were developed to determine self-absorption correction factors. The most accurate method to determine the correction factor is the experimental method (Aguiar *et al.*, 2006; Pilleyre *et al.*, 2006; El-Khatib *et al.*, 2014), where there is no need to make approximations. However, the experimental method is time-consuming and it is difficult to measure the full energy peak efficiency curve with sample preparation of different densities. So, the determination of the full energy peak efficiency is difficult by experimentally for the extended sources. To overcome these difficulties, Monte Carlo (MC) methods were used. The importance of such MC methods is that they enable one to quickly calculate a new efficiency value for changes in the measuring conditions. Different theoretical and MC approaches were used to calculate the full energy peak efficiency value including the effect of source self-absorption (Hardy *et al.*, 2002; Vargas *et al.*, 2002; Mostajaboddavati *et al.*, 2006; Abbas, 2007; Khater and Ebaid, 2008; Badawi *et al.*, 2012; Ababneh and Eyadeh, 2015). However, these methods required approximations and simplifications in the internal structure of the Ge crystal and source-detector geometries calculations (Shizuma *et al.*, 2016).

In addition, when the source is positioned close to the detector, a coincidence summing effect arise in those nuclides which emit cascade γ-rays. Many authors observed some strong deviation from experimental results without including

---

*Corresponding author: hechaohui@xjtu.edu.cn the effect of coincidence summing in the simulation (Rodenas *et al.*, 2003; Conti *et al.*, 2013). For the correction of such effect, the total efficiency is also required with the full energy peak efficiency. Debertin and Schötzig (1979) used the total efficiency (the ratio of the total number of counts observed to the number of photons emitted by the source) and calculated coincidence summing correction factor in measurements. Abbas *et al.* (2001) used the analytical approach to calculate the correction factor with total efficiency. Most of the authors used total efficiencies in the simulation for the calculation of coincidence summing correction factor (Wang *et al.*, 2002; Vidmar *et al.*, 2007; Ababneh and Eyadeh, 2015), and in recent years some authors used GEANT4 code and obtained good agreement with experimental results (Quintana and Montes, 2014; Giubrone *et al.*, 2016). But these approaches required elaborate work in its implementation, especially for the close geometry measurements and large volume samples (Lee *et al.*, 2008).

In this work, a simple and accurate method was developed in GEANT4 code to simulate the full energy peak efficiency ($\varepsilon_{\text{simu}}$) of a co-axial HPGe detector, including the self-absorption (SAF_{cal}) and coincidence summing (CSF_{cal}) correction factor of the extended environmental source. Simulated results were compared to experimental measurement for a typical cylindrical measuring geometry with different volumes in the energy range 60–1836 keV.

2 Materials and methods

The MC code GEANT4 (Khan *et al.*, 2018) can directly determine the energy deposited in the simulated volume of a detector, enabling the determination of $\varepsilon_{\text{simu}}$. The code provides a realistic and fast procedure for the accurate assessment of self-absorption correction in samples without any optimizations and approximations. It can handle complex source geometries with any sample density and composition. The code follows the history of each individual primary photon until its energy dissipated in the detector and produces secondary particles as a result of the photoelectric effect, Compton effect, and pair production interaction. Only the γ-rays, which deposit their full energy in the active volume of the detector, were considered for the evaluation of the full energy peak efficiency. The secondary electrons formed by photon interaction processes were also taken into consideration in the simulation. G4EMStandardPhysics class was used for the low-level γ-rays spectrometry in the simulation since the energy limit for the electromagnetic process is 10 to 100 TeV. Therefore, Ge X-rays of energy below 10 keV cannot be processed. The number of total histories (10^6 primary photons) was considered for the simulation to obtain a statistical uncertainty of no more than 0.1%. The $\varepsilon_{\text{simu}}$ values were obtained by the VMware workstation 15.0.1 using i5-3570K 3.40 GHz Intel core processor. The GEANT4 calculation CPU times, for 12 $\varepsilon_{\text{simu}}$ values, *i.e.* $\varepsilon_{\text{simu}}$ values for 12 γ-ray energies, were ~0.2 s for point sources and ~1 min for cylindrical sources.

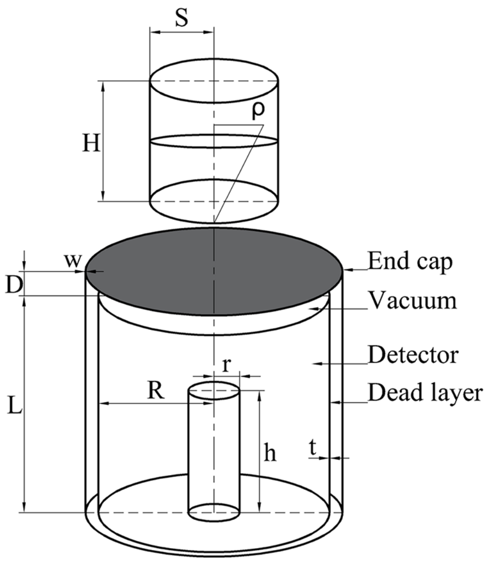

Fig. 1. Schematic of the source-detector.

The detector considered for MC simulation was a p-type coaxial HPGe detector (Canberra) with an active volume of approximately 18960.18 mm^3 (detector crystal with a length (l) of 89.7 mm, radius (r) of 34.95 mm, a core cavity with a height (h) of 80 mm and a radius (r) of 10 mm). The detector geometry was a closed-end coaxial and its relative efficiency at 1332 keV (^{60}Co) is 44.3%. The detector has an aluminum end-cap window of thickness (w) of 1 mm, placed at a distance (d) of 4 mm from the crystal and a nominal dead-layer thickness (t) of 0.7 mm. A scheme of the detector is shown in Figure 1. No information was available by the manufacturer about whether the Ge crystals had rounded edges. Sharp edges of the crystals were assumed in the simulation. A cylindrical beaker source of radius (S = 34.8 mm) filled with γ radionuclides aqueous solution of volumes V1 (100 mL) and V2 (500 mL) were used to obtain the full energy peak efficiency values. The radionuclides contained in the source solution are (^{241}Am, ^{85}Sr, ^{137}Cs, ^{109}Cd, ^{114}Sn, ^{88}Y, ^{57}Co, ^{139}Ce, ^{60}Co, ^{203}Hg), covering the energy range from 60 to 1836 keV. The cylindrical beaker source was placed in contact with the detector end-cap window. Besides the source self-absorption, it is also necessary to consider the photon attenuation in the germanium dead-layer and entrance aluminum window. The thickness of the dead layer has a large influence on the detector efficiency, especially for low energy range, where the low energy photons are increasingly absorbed. Regarding the effect of aluminum material surrounding the detector, there is the probability of low energy photons attenuation in this region. In our model, the radiation enters only through the upper face of the crystal and therefore, the sidewall thickness has no influence on full energy peak efficiency value.

The simulated full energy peak efficiency ($\varepsilon_{\text{simu}}$) is obtained from:

$$\varepsilon_{\text{simu}} = \frac{\text{Q}}{\text{M}}, \tag{1}$$

where $\varepsilon_{\text{simu}}$ is the full energy peak efficiency, Q is the number of events that deposit their full energy in the active detector volume, and M is the number of total simulated events for a given energy, E.

The calculated self-absorption correction factor ($\mathrm{SAF_{cal}}$) is obtained from:

$$\mathrm{SAF_{cal}} = \frac{\varepsilon^{*}_{\mathrm{simu}}}{\varepsilon_{\mathrm{simu}}}, \tag{2}$$

where $\varepsilon^{*}_{\mathrm{simu}}$ and $\varepsilon_{\mathrm{simu}}$ are the simulated efficiencies in the presence (water) and absence (vacuum) of the source attenuation, respectively.

In the absence of coincidence summing, the count rate ($\mathrm{N_1}$) is given by:

$$\mathrm{N_1} = \mathrm{A}\gamma_1\varepsilon_1\,, \tag{3}$$

where A is the source activity, γ_1 is the emission probability with energy E_1 and ε_1 is the peak efficiency for γ_1 with E_1.

If the energy of γ_1 is totally absorbed, the sum count rate is observed at an energy between E_1 and $E_1 + E_2$ and the event is lost from the full energy peak of γ_1. The observed full energy peak would become:

$$\mathrm{N}^{*}_1 = \mathrm{A}\gamma_1\varepsilon_1 \;-\; \mathrm{A}\gamma_1\varepsilon_1\varepsilon_{\mathrm{T2}}\,, \tag{4}$$

where N^{*}_1 is the count rate in the presence of coincidence summing, $\varepsilon_{\mathrm{T2}}$ is the total detection efficiency for γ_2. For a point source, the calculated coincidence summing correction factor ($\mathrm{CSF_{cal}}$) for γ_1 is given by:

$$\frac{\mathrm{N_1}}{\mathrm{N}^{*}_1} = \frac{1}{1-\varepsilon_{\mathrm{T2}}}, \tag{5}$$

or

$$\mathrm{CSF}^{a}_{\mathrm{cal}} \;=\; \frac{1}{1 \;-\; \varepsilon^{b}_{\mathrm{Tsimu}}}. \tag{6}$$

Similarly, for $\mathrm{CSF}^{b}_{\mathrm{cal}}$,

$$\mathrm{N_2} = \mathrm{A}\gamma_2\varepsilon_2, \tag{7}$$

$$\mathrm{N}^{*}_2 = \mathrm{A}\gamma_2\varepsilon_2 - \mathrm{A}\gamma_1\varepsilon_2\varepsilon_{\mathrm{T1}}, \tag{8}$$

$$\frac{\mathrm{N_2}}{\mathrm{N}^{*}_2} = \frac{1}{1-\frac{\gamma_1}{\gamma_2}\varepsilon_{\mathrm{T1}}}, \tag{9}$$

or

$$\mathrm{CSF}^{b}_{\mathrm{cal}} \;=\; \frac{1}{1 \;-\; \frac{\gamma_1}{\gamma_2}\,\varepsilon^{a}_{\mathrm{Tsimu}}}\,, \tag{10}$$

where $\mathrm{CSF}^{a}_{\mathrm{cal}}$ and $\mathrm{CSF}^{b}_{\mathrm{cal}}$ are the calculated coincidence summing correction factors, $\varepsilon^{a}_{\mathrm{Tsimu}}$ and $\varepsilon^{b}_{\mathrm{Tsimu}}$ are the simulated total efficiencies of 1173 keV (a) and 1332 keV (b) respectively, similarly for ^{88}Y. $\frac{\gamma_1}{\gamma_2}$ is the ratio between the emission probabilities for each multi γ-ray nuclide. Equations (6) and (10) show that the correction factors depend only on the total efficiencies and γ emission probabilities. The γ-ray emission probability (γ) values are listed in Table 1.

Table 1. Multi γ-ray nuclides with emission probability.

Radionuclide	E (keV)	γ (%)
^{60}Co	1173	99.90
	1332	99.98
^{88}Y	898	93.70
	1836	99.35

The coincidence summing effects become more complicated for the extended volume source. In this case, the correction factor not only depends on the peak and total efficiencies but also on the source volume and the differential efficiency distributions within the source. For a volume source, equations (3) and (4) have to be rewritten in a differential forms:

$$n_1(r)\rho\, d\rho = a(r)\gamma_1\varepsilon_1(r)\rho\, d\rho\,, \tag{11}$$

$$n^{*}_1(r)\rho\, d\rho = a(r)\gamma_1\varepsilon_1(r)\rho\, d\rho - \mathrm{a}(r)\gamma_1\varepsilon_1(r)\varepsilon_{\mathrm{T2}}(r)\rho\, d\rho\,. \tag{12}$$

$\rho\, d\rho$ is considered as a volume element, r denotes the position of $\rho\ d\rho$, $\varepsilon_1(r)$ and $\varepsilon_{\mathrm{T2}}(r)$ are the peak and total efficiencies at r, $n_1(r)\ \rho\ d\rho$ and $n^{*}_1(r)\rho\, d\rho$ represent $\mathrm{N_1}$ and N^{*}_1 respectively, but the γ-rays emitted from volume element $\rho\ d\rho$ at r in this case. $a(r)$ is the activity concentration at r. Integration on both sides of equations (11) and (12) over the source volume, we obtain:

$$\mathrm{N_1} = a(r)\gamma_1\!\int\!\varepsilon_1(r)\rho\, d\rho\,, \tag{13}$$

$$\mathrm{N}^{*}_1 = a(r)\gamma_1\!\int\!\varepsilon_1(r)\rho\, d\rho - \varepsilon_1(r)\varepsilon_{\mathrm{T2}}(r)\rho\, d\rho\,, \tag{14}$$

$$\frac{\mathrm{N_1}}{\mathrm{N}^{*}_1} = \frac{\int\varepsilon_1(r)\rho\, d\rho}{\int\varepsilon_1(r)(1-\varepsilon_{\mathrm{T2}}(r))\rho\, d\rho}\,, \tag{15}$$

or

$$\mathrm{CSF}^{a}_{\mathrm{cal}} = \frac{1}{\int\rho\,\varepsilon^{*}_{\mathrm{simu}}(1 \;-\; \varepsilon^{b}_{\mathrm{Tsimu}})d\rho\,/\int\rho\ \varepsilon^{*}_{\mathrm{simu}}\, d\rho}, \tag{16}$$

or

$$\mathrm{CSF}^{a}_{\mathrm{cal}} = \frac{1}{1-\int\rho\,\varepsilon^{*}_{\mathrm{simu}}\,\varepsilon^{b}_{\mathrm{simu}}\,d\rho\,/\int\rho\,\varepsilon^{*}_{\mathrm{simu}}\,d\rho}. \tag{17}$$

Similarly, for $\mathrm{CSF}^{b}_{\mathrm{cal}}$,

$$n_2(r)\rho\, d\rho = a(r)\gamma_2\varepsilon_2(r)\rho\, d\rho, \tag{18}$$

$$n^{*}_2(r)\rho\, d\rho = a(r)\gamma_2\varepsilon_2(r)\rho\, d\rho - \;a(r)\gamma_1\varepsilon_2(r)\varepsilon_{\mathrm{T1}}(r)\rho\, d\rho\,, \tag{19}$$

$$\mathrm{N}_2 = a(r)\gamma_2 \int \varepsilon_2(r)\rho d\rho, \tag{20}$$

$$\mathrm{N}_2^* = a(r)\gamma_2 \int \varepsilon_2(r)\rho\, d\rho - \frac{\gamma_1}{\gamma_2}\varepsilon_2(r)\varepsilon_{\mathrm{T1}}(r)\rho\, d\rho, \tag{21}$$

$$\frac{\mathrm{N}_2}{\mathrm{N}_2^*} = \frac{\int \varepsilon_2(r)\rho\, d\rho}{\int \varepsilon_2(r)(1-\frac{\gamma_1}{\gamma_2}\varepsilon_{\mathrm{T1}}(r))\rho\, d\rho}, \tag{22}$$

or

$$\mathrm{CSF}^b_{\mathrm{cal}} = \frac{1}{\int \rho\, \varepsilon^*_{\mathrm{simu}}(1 - \frac{\gamma_1}{\gamma_2}\varepsilon^a_{\mathrm{Tsimu}})d\rho \,/ \int \rho\, \varepsilon^*_{\mathrm{simu}}\, d\rho}, \tag{23}$$

or

$$\mathrm{CSF}^b_{\mathrm{cal}} = \frac{1}{1 - \int p\varepsilon^*_{\mathrm{simu}} \frac{\gamma_1}{\gamma_2}\varepsilon^a_{\mathrm{Tsimu}})\, dp \,/ \int p\varepsilon^*_{\mathrm{simu}}\, dp}, \tag{24}$$

or, as a summation, equations (17) and (24) can be written as:

$$\mathrm{CSF}^a_{\mathrm{cal}} = \frac{1}{1 - [\Sigma\rho_i\varepsilon^*_{\mathrm{simu}}\varepsilon^b_{\mathrm{Tsimu}})d\rho \,/\, \Sigma\rho_i\varepsilon^*_{\mathrm{simu}}\, d\rho]}, \tag{25}$$

$$\mathrm{CSF}^b_{\mathrm{cal}} = \frac{1}{1 - [\Sigma\rho_i\varepsilon^*_{\mathrm{simu}}\frac{\gamma_1}{\gamma_2}\varepsilon^a_{\mathrm{Tsimu}})d\rho \,/\, \Sigma\rho_i\varepsilon^*_{\mathrm{simu}}\, d\rho]}, \tag{26}$$

where ρ_i is the point source positions from the detector axis in volume source. Equations (25) and (26) can be written as:

$$\mathrm{CSF}^a_{\mathrm{cal}} = \frac{1}{1 - \langle \mathrm{J}_1 \rangle}. \tag{27}$$

For H_1,

$$\langle \mathrm{J}_{1H_1} \rangle = \Sigma\rho_i\, \varepsilon^*_{\mathrm{simu}}\, \varepsilon^b_{\mathrm{Tsimu}}\, d\rho \,/\, \Sigma\rho_i\, \varepsilon^*_{\mathrm{simu}}\, d\rho. \tag{28}$$

For the whole volume source height,

$$\langle \mathrm{J}_1 \rangle = \frac{\sum_{i=1}^{2} \mathrm{J}_{1H_i}}{2}, \tag{29}$$

where H_i are the different distances from the beaker bottom. Similarly,

$$\mathrm{CSF}^b_{\mathrm{cal}} = \frac{1}{1 - \langle \mathrm{J}_2 \rangle}, \tag{30}$$

$$\langle \mathrm{J}_{2H_1} \rangle = \Sigma\rho_i\, \varepsilon^*_{\mathrm{simu}} \frac{\gamma_1}{\gamma_2} \varepsilon^a_{\mathrm{Tsimu}}\, d\rho \,/\, \Sigma\rho_i\, \varepsilon^*_{\mathrm{simu}}\, d\rho, \tag{31}$$

$$\langle \mathrm{J}_2 \rangle = \frac{\sum_{i=1}^{2} \mathrm{J}_{2H_i}}{2}, \tag{32}$$

where $\langle \mathrm{J}_1 \rangle$ and $\langle \mathrm{J}_2 \rangle$are the 10-point integration of efficiencies for each nuclide. To calculate the coincidence summing correction for both source volumes, first, the beaker volume is divided into two volumes (H_1 and H_2) and then further subdivided into 5 volume elements (ρ_i) for each (H_1 and H_2). Four single nuclide point sources with photon energies (^{60}Co (1173 keV, 1332 keV) and ^{88}Y (898 keV, 1898 keV)) were placed at 10 positions within the source volume with two different distances (H_1 and H_2) from the beaker bottom. To get $\mathrm{J}_{1\mathrm{H}_1}$ for 898 or 1173 keV, first computed the $\varepsilon^*_{\mathrm{simu}}$ and $\varepsilon^b_{\mathrm{Tsimu}}$ (1836 or 1332 keV) values at 5 different positions in the source volume and then computed the 5-point integration (*i.e.*, multiplied each value by ρ_i, summed them, and divided by the sum of the $\rho_i\varepsilon^*_{\mathrm{simu}}$). Similarly, calculated $\mathrm{J}_{1\mathrm{H}_2}$(5-point integration of efficiencies) at height H_2 and averaged them to get $\langle \mathrm{J}_1 \rangle$ at 10 volume elements. The $\varepsilon^*_{\mathrm{simu}}$ and $\varepsilon_{\mathrm{Tsimu}}$values does not change with the further subdivision of the beaker volume. Similarly, computed the $\varepsilon^*_{\mathrm{simu}}$ and $\varepsilon^a_{\mathrm{Tsimu}}$(898 or 1173 keV) values at 10 different positions to obtain $\langle \mathrm{J}_2 \rangle$ for 1836 or 1332 keV.

The true simulated full energy peak efficiency ($\varepsilon^o_{\mathrm{simu}}$) is obtained from:

$$\varepsilon^o_{\mathrm{simu}} = \varepsilon^*_{\mathrm{simu}} \times \mathrm{CSF}_{\mathrm{cal}}\,. \tag{33}$$

3 Results and discussion

3.1 Analysis of self-absorption correction factor

The full energy peak efficiency was simulated for a cylindrical water composition source of density ($\rho = 1$ g/cm^3) with two different volumes. First, the simulated result was obtained without source self-absorption of the source matrix (water) and there was no attenuation of a γ-ray photon from the source matrix but attenuated from the source container material. As given in Tables 2 and 3, the $\varepsilon_{\mathrm{simu}}$ results without source self-absorption are compared with the experimental full energy peak efficiency ($\varepsilon_{\mathrm{Exp}}$) values. Obviously, the non-inclusion of the source self-absorption caused an increase in $\varepsilon_{\mathrm{simu}}$ values. For various source volumes, large deviations in $\varepsilon_{\mathrm{simu}}$ values without source self-absorption were observed with the experimental results. So to obtain the correct simulated results, the source self-absorption must be taken into consideration. Tables 2 and 3 show the $\mathrm{SAF}_{\mathrm{cal}}$ values for different source volumes. These tables clearly show the effect of the source self-absorption on the $\varepsilon_{\mathrm{simu}}$ value, especially for the low photon energy. The $\mathrm{SAF}_{\mathrm{cal}}$ value is somewhat great and it's more effective for the low photon energy. The relative deviations (RD) are somewhat greater at high energies for both source volumes. Tables 2 and 3 show good agreement between simulated ($\varepsilon^*_{\mathrm{simu}}$) and experimental ($\varepsilon_{\mathrm{Exp}}$) results with RD less than 2% at low energies due to the inclusion of $\mathrm{SAF}_{\mathrm{cal}}$.

For the extended sources, different samples with different chemical composition and density caused significant variations in the full energy peak efficiency value. But for most environmental samples, the full energy peak efficiency with source self-absorption greatly depends on the density of the samples. To observe the sample density effect on the full energy peak efficiency value, we simulated the full energy peak efficiency value for four samples with different density (0.8, 1,

Table 2. Relative deviation between experimental and simulated (ε^{*}_{simu}) full energy peak efficiency values with self-absorption correction factor for V1.

E (keV)	ε_{Exp}	ε_{simu}	SAF_{cal}	ε^{*}_{simu}	RD (%)
60	0.02400	0.02947	0.82	0.02443	1.6
88	0.06933	0.08800	0.79	0.06970	0.5
122	0.07520	0.08995	0.84	0.07578	0.6
166	0.07093	0.08646	0.82	0.07124	0.4
279	0.05547	0.06638	0.84	0.05575	0.5
392	0.04320	0.04973	0.86	0.04321	0.0
514	0.03467	0.04094	0.85	0.03513	1.4
662	0.03093	0.03320	0.93	0.03096	0.0
898	0.02347	0.02500	0.88	0.02203	−6.3
1173	0.01920	0.01900	0.94	0.01788	−7.8
1332	0.01867	0.01800	0.95	0.01722	−8.1
1836	0.01493	0.01430	0.96	0.01382	−7.9

Table 3. Relative deviation between experimental and simulated (ε^{*}_{simu}) full energy peak efficiency values with self-absorption correction factor for V2.

E (keV)	ε_{Exp}	ε_{simu}	SAF_{cal}	ε^{*}_{simu}	RD (%)
60	0.00696	0.01281	0.53	0.00690	−0.8
88	0.01607	0.03253	0.50	0.01631	1.8
122	0.02089	0.03728	0.56	0.02107	0.9
166	0.02036	0.03462	0.59	0.02064	1.4
279	0.01446	0.02634	0.55	0.01468	1.3
392	0.01232	0.01984	0.63	0.01256	1.6
514	0.01018	0.01679	0.61	0.01032	1.9
662	0.00964	0.01441	0.66	0.00965	0.1
898	0.00750	0.01134	0.63	0.00718	−4.4
1173	0.00719	0.00980	0.69	0.00680	−5.7
1332	0.00643	0.00880	0.69	0.00609	−5.5
1836	0.00536	0.00719	0.80	0.00576	6.9

1.5 and 1.9 g/cm^3). As shown in Tables 4 and 5, the comparison of the simulated results for various samples volumes, show the dependence of ε^{*}_{simu} value on different sample density. The tables show that when the density of the sample increases the ε^{*}_{simu} value decreases because the minimum number of γ-rays scattered in the samples itself at greater density.

3.2 Analysis of coincidence summing correction factor

For the energy range (60 to 662 keV), a good agreement was achieved with SAF_{cal}. However, for the high energy range (898 to 1836 keV), maximum discrepancies were obtained due to the non-inclusion of coincidence summing effect in ε^{*}_{simu} values. In the case of extended sources, the ε_{Tsimu} value needs to be taken into account to find CSF_{cal} for ^{60}Co and ^{88}Y. Table 6 shows the 10-point integration of efficiency values obtained with GEANT4 for the extended volumetric sources.

The 10-point integration of efficiency values obtained with our simulation approach is simple and precise to be used to calculate the coincidence summing correction factor. The values of the correction factor for ^{60}Co and ^{88}Y are shown in Table 7. The CSF_{cal} is independent of the detector count rate but it is strongly dependent on the full energy peak and total efficiency. By comparison, there is an inverse relationship between $\langle J \rangle$ and CSF_{cal} values for nuclides ^{60}Co and ^{88}Y. Results indicated that the CSF_{cal} also depends on the different source volume. Table 7 shows that the CSF_{cal} decreases with the source volume, which means that the probability of such summing effects decreases with increasing of the source to detector distance.

The true ε^{o}_{simu} values were obtained by applying the CSF_{cal} in the simulation for nuclide ^{60}Co and ^{88}Y. Table 8 shows a good agreement with the experimental results, with discrepancies less than 2% for both extended volumetric sources.

Table 4. Variation of the full energy peak efficiency value with density for V1.

		Kerosene	Water	Nitric acid	Potassium chloride
Density p (g/cm^3)		0.8	1	1.5	1.9
E (keV)	ε_{Exp}	$\varepsilon^*_{\text{simu}}$			
60	0.02400	0.02630	0.02443	0.01850	0.01321
88	0.06933	0.07140	0.06970	0.06540	0.06120
122	0.07520	0.07730	0.07578	0.07200	0.06703
166	0.07093	0.07330	0.07124	0.06750	0.06400
279	0.05547	0.05690	0.05575	0.05230	0.05010
392	0.04320	0.04460	0.04321	0.03930	0.03690
514	0.03467	0.03690	0.03513	0.03410	0.03320
662	0.03093	0.03230	0.03096	0.03010	0.02960
898	0.02347	0.02350	0.02200	0.02010	0.01850
1173	0.01920	0.01930	0.01788	0.01520	0.01290
1332	0.01867	0.01870	0.01722	0.01430	0.01220
1836	0.01493	0.01550	0.01382	0.01200	0.01020

Table 5. Variation of the full energy peak efficiency value with density for V2.

		Kerosene	Water	Nitric acid	Potassium chloride
Density p (g/cm^3)		0.8	1	1.5	1.9
E (keV)	ε_{Exp}	$\varepsilon^*_{\text{simu}}$			
60	0.00696	0.00706	0.00690	0.00440	0.00260
88	0.01607	0.01790	0.01631	0.01490	0.01240
122	0.02089	0.02210	0.02107	0.01850	0.01650
166	0.02036	0.02190	0.02064	0.01810	0.01600
279	0.01446	0.01590	0.01468	0.01360	0.01220
392	0.01232	0.01390	0.01256	0.01200	0.01100
514	0.01018	0.01160	0.01032	0.00993	0.00979
662	0.00964	0.00979	0.00965	0.00951	0.00939
898	0.00750	0.00729	0.00718	0.00691	0.00661
1173	0.00719	0.00701	0.00680	0.00655	0.00631
1332	0.00643	0.00621	0.00609	0.00585	0.00561
1836	0.00536	0.00591	0.00576	0.00541	0.00512

4 Conclusions

GEANT4 simulation toolkit was used to simulate the full energy peak efficiency of a coaxial HPGe detector for theextended volumetric sources. The self-absorption correction factors were calculated and obtained accurate full energy peak efficiency values for the low energy range. The simulation was performed and observed the dependence of the full energy peak efficiency value on different sample densities. A new method was used in GEANT4 to calculate the coincidence summing correction factors and obtained accurate simulated results; the discrepancies between the experimental and simulated efficiencies were found less than 2%. The proposed simulated method avoids the preparation of the great variety of radioactive samples with several isotopes and has added the advantages to improve the detection efficiencies for the measurement of the activity of various samples.

Table 6. Calculated 10-point integration of efficiency values for different source volumes.

		V1	V2
E (keV)	10-point integration of efficiencies		
898	⟨J_1⟩	0.07927	0.05546
1173	⟨J_1⟩	0.08262	0.05988
1332	⟨J_2⟩	0.08651	0.06200
1836	⟨J_2⟩	0.08924	0.07087

Table 7. Calculated coincidence summing correction from 10-point integration efficiency values.

Volumes	Radionuclide	E (keV)	CSF_{cal}
V1	^{60}Co	1173	1.09
		1332	1.09
	^{88}Y	898	1.08
		1836	1.09
V2	^{60}Co	1173	1.06
		1332	1.06
	^{88}Y	898	1.05
		1836	1.07

Table 8. Comparison of experimental and simulated full energy peak efficiency values with CSF_{cal}.

Volumes	Radionuclide	E (keV)	ε_{Exp}	ε^{*}_{simu}	CSF_{cal}	ε^{o}_{simu}	RD (%)
V1	^{60}Co	1173	0.01920	0.01788	1.09	0.01950	1.5
		1332	0.01867	0.01722	1.09	0.01880	1.0
	^{88}Y	898	0.02347	0.02200	1.08	0.02380	1.7
		1836	0.01493	0.01382	1.09	0.01510	1.3
V2	^{60}Co	1173	0.00719	0.00680	1.06	0.00721	0.2
		1332	0.00643	0.00609	1.06	0.00646	0.4
	^{88}Y	898	0.00750	0.00718	1.05	0.00754	0.5
		1836	0.00536	0.00576	1.07	0.00539	0.5

Acknowledgments. This work at Xian Jiaotong University was fully supported by the Chinese government. The authors would like to thank the entire staff of the Nuclear Science and Technology department for the very valuable information in the completion of this work.

References

Ababneh AM, Eyadeh MM. 2015. Coincidence summing corrections in HPGe gamma-ray spectrometry for Marinelli-beakers geometry using peak to total (P/T) calibration. *J. Radiat. Res. Appl. Sci.* 8: 323–327.

Abbas MI. 2007. Direct mathematical method for calculating full-energy peak efficiency and coincidence corrections of HPGe detectors for extended sources. *Nucl. Instr. Meth. Phys. Res. B* 256: 554–557.

Abbas MI, Selim YS, Bassiouni M. 2001. HPGe detector photopeak efficiency calculation including self-absorption and coincidence corrections for cylindrical sources using compact analytical expressions. *Radiat. Phys. Chem.* 61: 429–431.

Aguiar JC, Galiano E, Fernandez J. 2006. Peak efficiency calibration for attenuation corrected cylindrical sources in gamma ray spectrometry by the use of a point source. *Appl. Radiat. Isot.* 64: 1643–1647.

Badawi MS, Gouda MM, Nafee SS, El-Khatib AM, El-Mallah EA. 2012. New analytical approach to calibrate the co-axial HPGe detectors including correction for source matrix self-attenuation. *Appl. Radiat. Isot.* 70: 2661–2668.

Budjáš D, Heisel M, Maneschg W, Simgen H. 2009. Optimisation of the MC-model of a *p*-type Ge-spectrometer for the purpose of efficiency determination. *Appl. Radiat. Isot.* 67: 706–710.

Conti C, Salinas I, Zylberberg H. 2013. A detailed procedure to simulate an HPGe detector with MCNP5. *Prog. Nucl. Energy* 66: 35–40.

Debertin K, Schötzig U. 1979. Coincidence summing corrections in Ge (Li)-spectrometry at low source-to-detector distances. *Nucl. Instr. Meth. Phys. Res.* 158: 471–477.

El-Khatib AM, Thabet AA, Elzaher MA, Badawi MS, Salem BA. 2014. Study on the effect of the self-attenuation coefficient on γ-ray detector efficiency calculated at low and high energy regions. *Nucl. Eng. Technol.* 46: 217–224.

Giubrone G, Ortiz J, Gallardo S, Martorell S, Bas M. 2016. Calculation of coincidence summing correction factors for an HPGe detector using GEANT4. *J. Environ. Radioact.* 158: 114–118.

Hardy J, Iacob V, Sanchez-Vega M, Effinger R, Lipnik P, Mayes V, Willis D, Helmer R. 2002. Precise efficiency calibration of an HPGe detector: Source measurements and Monte Carlo calculations with sub-percent precision. *Appl. Radiat. Isot.* 56: 65–69.

Helmer R, Nica N, Hardy J, Iacob V. 2004. Precise efficiency calibration of an HPGe detector up to 3.5 MeV, with measurements and Monte Carlo calculations. *Appl. Radiat. Isot.* 60: 173–177.

Hurtado S, Garcıa-León M, Garcıa-Tenorio R. 2004. GEANT4 code for simulation of a germanium gamma-ray detector and its application to efficiency calibration. *Nucl. Instr. Meth. Phys. Res. A* 518: 764–774.

Khan W, Zhang Q, He C, Saleh M. 2018. Monte Carlo simulation of the full energy peak efficiency of an HPGe detector. *Appl. Radiat. Isot.* 131: 67–70.

Khater A, Ebaid Y. 2008. A simplified gamma-ray self-attenuation correction in bulk samples. *Appl. Radiat. Isot.* 66: 407–413.

Lee M, Park TS, Woo J-K. 2008. Coincidence summing effects in gamma-ray spectrometry using a Marinelli beaker. *Appl. Radiat. Isot.* 66: 799–803.

Mostajaboddavati M, Hassanzadeh S, Faghihian H. 2006. Efficiency calibration and measurement of self-absorption correction for environmental gamma-spectroscopy of soil samples using Marinelli beaker. *J. Radioanal. Nucl. Chem.* 268: 539–544.

Pilleyre T, Sanzelle S, Miallier D, Fain J, Courtine F. 2006. Theoretical and experimental estimation of self-attenuation corrections in determination of 210Pb by γ-spectrometry with well Ge detector. *Radiat. Meas.* 41: 323–329.

Quintana B, Montes C. 2014. Summing-coincidence corrections with Geant4 in routine measurements by γ spectrometry of environmental samples. *Appl. Radiat. Isot.* 87: 390–393.

Rodenas J, Pascual A, Zarza I, Serradell V, Ortiz J, Ballesteros L. 2003. Analysis of the influence of germanium dead layer on detector calibration simulation for environmental radioactive samples using the Monte Carlo method. *Nucl. Instr. Meth. Phys. Res. A* 496: 390–399.

Shizuma K, Oba Y, Takada M. 2016. A practical method for determining γ-ray full-energy peak efficiency considering coincidence-summing and self-absorption corrections for the measurement of environmental samples after the Fukushima reactor accident. *Nucl. Instr. Meth. Phys. Res. B* 383: 183–190.

Vargas MJ, Timón AF, Díaz NC, Sánchez DP. 2002. Monte Carlo simulation of the self-absorption corrections for natural samples in gamma-ray spectrometry. *Appl. Radiat. Isot.* 57: 893–898.

Vidmar T, Korun M, Vodenik B. 2007. A method for calculation of true coincidence summing correction factors for extended sources. *Appl. Radiat. Isot.* 65: 243–246.

Wang Z, Kahn B, Valentine JD. 2002. Efficiency calculation and coincidence summing correction for germanium detectors by Monte Carlo simulation. *IEEE Trans. Nucl. Sci.* 49: 1925–1931.

Cite this article as: Khan W, He C, Cao Y. 2019. Calculation of self-absorption and coincidence summing correction factors for the extended sources using GEANT4. *Radioprotection* 54(2): 133–140